arXiv:1512.03281v1 [hep-ex] 10 Dec 2015

New results on the XYZ states from Belle experiment

Chang-Zheng Yuan for the Belle Collaboration[1,a)]

[1]*Institute of High Energy Physics, Chinese Academy of Sciences, Beijing 100049, China*

[a)]Corresponding author: yuancz@ihep.ac.cn

Abstract. We review the results on the XYZ states from the Belle experiment, including the measurement of inclusive hadronic cross sections and exclusive cross sections in e^+e^- annihilation and the Z_b states in the bottomonium energy region; and the study of the Y states and the Z_c states in charmonium energy region.

INTRODUCTION

Many charmonium and charmonium-like states were discovered at B-factories in the first decade of the 21st century followed by similar discoveries in the bottomonium and bottomniumlike states [1]. Whereas some of these are good quarkonium candidates, as predicted in different models, many states have exotic properties, which may indicate that exotic states, such as multi-quark, molecule, hybrid, or hadron-quarkonium, have been observed [2]. In such studies, the Belle experiment [3] at the KEKB asymmetric-energy e^+e^- collider (3.5 GeV e^+ and 8.0 GeV e^-) [4] played a leading role.

The Belle detector is a large-solid-angle magnetic spectrometer that consists of a silicon vertex detector, a 50-layer central drift chamber, an array of aerogel threshold Cherenkov counters, a barrel-like arrangement of time-of-light scintillation counters, and an electromagnetic calorimeter comprised of CsI(Tl) crystals located inside a super-conducting solenoid coil that provides a 1.5T magnetic field. An iron flux return located outside of the coil is instrumented to detect $K^0_{\rm L}$ mesons and to identify muons.

Belle experiment accumulated 1014 fb^{-1} data at different Υ peaks and at the continuum energies nearby. The main data samples are summarized in Table 1.

TABLE 1. Data samples collected at Belle experiment.

$\sqrt{s}$ (GeV)	$\mathcal{L}$ (fb^{-1})	description of the sample
9.460	6	$(102 \pm 2) \times 10^6$ $\Upsilon(1S)$ events
10.023	25	$(158 \pm 4) \times 10^6$ $\Upsilon(2S)$ events
10.355	3	$(11.0 \pm 0.3) \times 10^6$ $\Upsilon(3S)$ events
10.580	702	$(772 \pm 10) \times 10^6$ $\Upsilon(4S)$ events
10.867	121	$(7.1 \pm 1.3) \times 10^6$ $\Upsilon(5S)$ events
10.520	89	off resonance
10.63-11.05	28	$\Upsilon(5S)$ scan at 83 energies

BOTTOMONIUM and BOTTOMONIUMLIKE STATES

With the 83 scan data points for $\sqrt{s}$ = 10.63–11.05 GeV, and the larger data sample at the $\Upsilon(5S)$ peak, we measured the inclusive cross section of $e^+e^- \to b\bar{b}$ [5], the exclusive cross sections of $e^+e^- \to \pi^+\pi^-\Upsilon(nS)$ [5], $\pi^+\pi^- h_b(nP)$ [7],

clear resonant structures are observed which correspond to the $5S$ and $6S$ bottomonium states. The intermediate states in the three-body decays of $\Upsilon(5S) \to \pi^+\pi^-\Upsilon(nS)$ [6], $\pi^+\pi^- h_b(nP)$, as well as $B^{(*)}\bar{B}^{(*)}\pi$ are studied, information on charged bottomonium states, $Z_b(10610)$ and $Z_b(10650)$, are obtained.

The data consist of 121.4 fb^{-1} at $\sqrt{s} = 10.865$ GeV; approximately 1 fb^{-1} at each of the 22 energy points between 10.63 and 11.02 GeV; and 50 pb^{-1} at each of 61 points taken in 5 MeV steps between 10.75 and 11.05 GeV. The non-resonant $q\bar{q}$ continuum ($q \in \{u, d, s, c\}$) background is obtained using a 1.03 fb^{-1} data sample taken at $\sqrt{s} = 10.52$ GeV.

R_b Measurement

This measurement was done with all the data samples above 10.63 GeV. The reduced $e^+e^- \to b\bar{b}$ cross section is defined as $R_b \equiv \frac{\sigma(e^+e^- \to b\bar{b})}{\sigma^0(e^+e^- \to \mu^+\mu^-)}$, where the denominator is the Born cross section of $e^+e^- \to \mu^+\mu^-$. In this analysis [5], we select hadronic events and subtract the non-$b\bar{b}$ background and initial state radiation (ISR) produced narrow bottomonium states, then do efficiency correction. The resulting R_b and the fit with $\Upsilon(5S)$ and $\Upsilon(6S)$ are shown in Fig. 1(left). From the fit to R_b, we find $M_{10860} = (10881.8^{+1.0}_{-1.1} \pm 1.2)$ MeV/c^2, $\Gamma_{10860} = (48.5^{+1.9\ +2.0}_{-1.8\ -2.8})$ MeV, $M_{11020} = (11003.0 \pm 1.1^{+0.9}_{-1.0})$ MeV/c^2, $\Gamma_{11020} = (39.3^{+1.7\ +1.3}_{-1.6\ -2.4})$ MeV, and $\phi_{11020} - \phi_{10860} = (-1.87^{+0.32}_{-0.51} \pm 0.16)$ rad. The fit results depend strongly on the parametrization of the line shape and the fitting range as there are many bottom meson pair thresholds in this energy region.

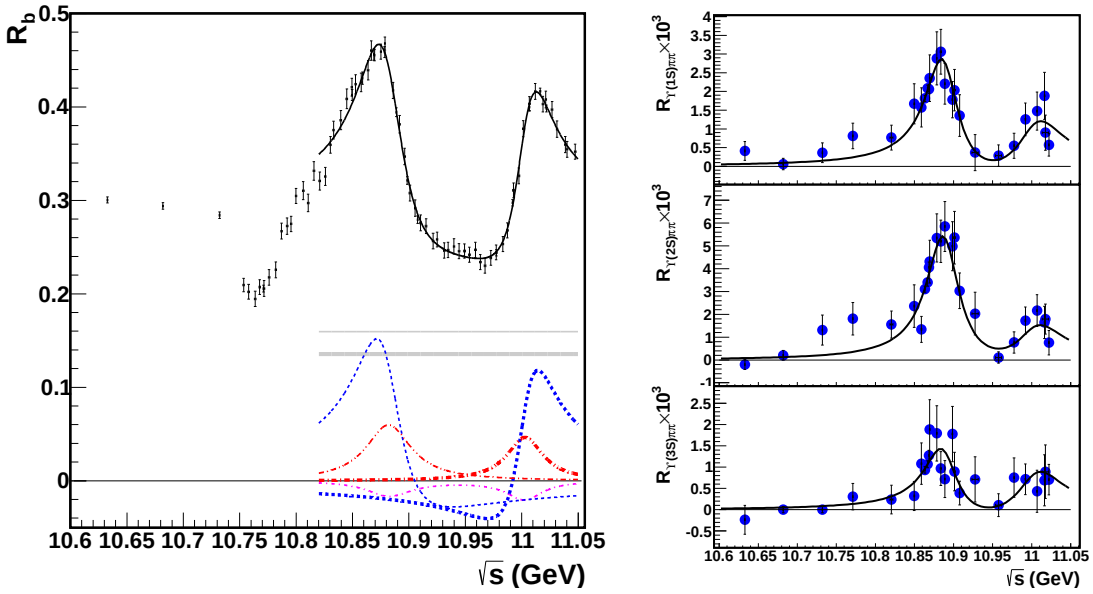


FIGURE 1. R_b data with components of fit (left) and $e^+e^- \to \pi^+\pi^-\Upsilon(nS)$ data (right) for $\Upsilon(1S)$ (top), $\Upsilon(2S)$ (center), and $\Upsilon(3S)$ (bottom), and the fit with coherent sum of two Breit-Wigner functions. Error bars are statistical only.

$e^+e^- \to \pi^+\pi^-\Upsilon(nS)$ and $Z_b \to \pi^\pm\Upsilon(nS)$

The cross sections of $e^+e^- \to \pi^+\pi^-\Upsilon(nS)$ (n = 1, 2, 3) at $\Upsilon(5S)$ peak and 22 energy points between 10.63 and 11.02 GeV with approximately 1 fb^{-1} each are measured.

Candidate $\Upsilon(nS)[\to \mu^+\mu^-]\pi^+\pi^-$ events are selected for the measurement. Figure 1(right) shows the $R_{\pi^+\pi^-\Upsilon(nS)} \equiv \sigma(e^+e^- \to \pi^+\pi^-\Upsilon(nS))/\sigma^0(e^+e^- \to \mu^+\mu^-)$. The cross sections are fit for the masses and widths of the $\Upsilon(5S)$ and $\Upsilon(6S)$ resonances. Unlike R_b, which includes a large non-resonant $b\bar{b}$ component, it is found that $e^+e^- \to \pi^+\pi^-\Upsilon(nS)$ is dominated by the two resonances. With $e^+e^- \to \pi^+\pi^-\Upsilon(nS)$, we measure $M_{10860} = (10891.1 \pm 3.2^{+0.6}_{-1.5})$ MeV/c^2

and $\Gamma_{10860} = (53.7^{+7.1\,+0.9}_{-5.6\,-5.4})$ MeV, and report the first measurements $M_{11020} = (10987.5^{+6.4\,+9.0}_{-2.5\,-2.1})$ MeV/c^2, $\Gamma_{11020} = (61^{+9\,\,+2}_{-19\,-20})$ MeV, and the relative phase $\phi_{11020} - \phi_{10860} = (-1.0 \pm 0.4\,^{+1.0}_{-0.1})$ rad.

The large statistics at the $\Upsilon(5S)$ peak make a study of the intermediate states of $e^+e^- \to \pi^+\pi^-\Upsilon(nS)$ possible [6]. After all the selections, we are left with 1905, 2312, and 635 candidate events for the $\pi^+\pi^-\Upsilon(1S)$, $\pi^+\pi^-\Upsilon(2S)$, and $\pi^+\pi^-\Upsilon(3S)$ final states, respectively. We performed a full amplitude analysis of three-body $e^+e^- \to \pi^+\pi^-\Upsilon(nS)$ transitions and determined the relative fractions of various quasi-two-body components of the three-body amplitudes as well as the spin and parity of the two observed Z_b states. The favored quantum numbers are $J^P = 1^+$ for both $Z_b(10610)$ and $Z_b(10650)$ states while the alternative $J^P = 1^-$ and $J^P = 2^\pm$ combinations are rejected at confidence levels exceeding 6 standard deviations.

Results of the amplitude analysis are summarized in Table 2, where fractions of individual quasi-two-body modes, masses and widths of the two Z_b states, the relative phase, ϕ_Z, between the two Z_b amplitudes and fraction $c_{Z_{10610}}/c_{Z_{10650}}$ of their amplitudes are given.

TABLE 2. Summary of results of fits to $\pi^+\pi^-\Upsilon(nS)$ events in the signal regions.

Parameter	$\pi^+\pi^-\Upsilon(1S)$	$\pi^+\pi^-\Upsilon(2S)$	$\pi^+\pi^-\Upsilon(3S)$
$f_{Z_b^\mp(10610)\pi^\pm}$, %	$4.8 \pm 1.2^{+1.5}_{-0.3}$	$18.1 \pm 3.1^{+4.2}_{-0.3}$	$30.0 \pm 6.3^{+5.4}_{-7.1}$
$Z_b(10610)$ mass, MeV/c^2	$10608.5 \pm 3.4^{+3.7}_{-1.4}$	$10608.1 \pm 1.2^{+1.5}_{-0.2}$	$10607.4 \pm 1.5^{+0.8}_{-0.2}$
$Z_b(10610)$ width, MeV	$18.5 \pm 5.3^{+6.1}_{-2.3}$	$20.8 \pm 2.5^{+0.3}_{-2.1}$	$18.7 \pm 3.4^{+2.5}_{-1.3}$
$f_{Z_b^\mp(10650)\pi^\pm}$, %	$0.87 \pm 0.32^{+0.16}_{-0.12}$	$4.05 \pm 1.2^{+0.95}_{-0.15}$	$13.3 \pm 3.6^{+2.6}_{-1.4}$
$Z_b(10650)$ mass, MeV/c^2	$10656.7 \pm 5.0^{+1.1}_{-3.1}$	$10650.7 \pm 1.5^{+0.5}_{-0.2}$	$10651.2 \pm 1.0^{+0.4}_{-0.3}$
$Z_b(10650)$ width, MeV	$12.1^{+11.3+2.7}_{-4.8-0.6}$	$14.2 \pm 3.7^{+0.9}_{-0.4}$	$9.3 \pm 2.2^{+0.3}_{-0.5}$
ϕ_Z, degrees	$67 \pm 36^{+24}_{-52}$	$-10 \pm 13^{+34}_{-12}$	$-5 \pm 22^{+15}_{-33}$
$c_{Z_b(10650)}/c_{Z_b(10610)}$	$0.40 \pm 0.12^{+0.05}_{-0.11}$	$0.53 \pm 0.07^{+0.32}_{-0.11}$	$0.69 \pm 0.09^{+0.18}_{-0.07}$
$f_{\Upsilon(nS)f_2(1270)}$, %	$14.6 \pm 1.5^{+6.3}_{-0.7}$	$4.09 \pm 1.0^{+0.33}_{-1.0}$	–
$f_{\Upsilon(nS)(\pi^+\pi^-)_S}$, %	$86.5 \pm 3.2^{+3.3}_{-4.9}$	$101.0 \pm 4.2^{+6.5}_{-3.5}$	$44.0 \pm 6.2^{+1.8}_{-4.3}$
$f_{\Upsilon(nS)f_0(980)}$, %	$6.9 \pm 1.6^{+0.8}_{-2.8}$	–	–

$e^+e^- \to \pi^+\pi^- h_b(nP)$ and $Z_b \to \pi^\pm h_b(nP)$

We measure $e^+e^- \to \pi^+\pi^- h_b(nP)$ (n =1, 2) with on-resonance $\Upsilon(5S)$ data of 121.4 fb^{-1} taken in three closely spaced energy points near 10.866 GeV, and energy scan data in the range from about 10.77 to 11.02 GeV taken at 19 points of about 1 fb^{-1} each.

The processes $e^+e^- \to \pi^+\pi^- h_b(nP)$ are reconstructed inclusively using the missing mass of $\pi^+\pi^-$ pairs, $M^{\rm miss}_{\pi^+\pi^-} = \sqrt{(\sqrt{s} - E^*_{\pi^+\pi^-})^2 - p^{*2}_{\pi^+\pi^-}}$, where $E^*_{\pi^+\pi^-}$ and $p^*_{\pi^+\pi^-}$ are the energy and momentum of the $\pi^+\pi^-$ pair measured in the center-of-mass (CM) frame.

The resulting cross sections are shown in Fig. 2. We perform a simultaneous fit to the energy dependence of the $e^+e^- \to \pi^+\pi^- h_b(nP)$ (n = 1, 2) cross sections. The fit function is a coherent sum of two Breit-Wigner (BW) amplitudes and (optionally) a constant with an energy continuum contribution:

$$A_n \; f(s)\, |BW(s, M_5, \Gamma_5) + a\, e^{i\phi} BW(s, M_6, \Gamma_6) + b\, e^{i\delta}|^2, \tag{1}$$

where $f(s)$ is the phase space function, which is calculated numerically taking into account the measured Z_b line shape, $BW(s, M, \Gamma)$ is a BW amplitude $BW(s, M, \Gamma) = M\Gamma/(s - M^2 + iM\Gamma)$. The parameters A_1, A_2, M_5, Γ_5, M_6, Γ_6, a, ϕ and (optionally) b, δ are floated in the fit.

We find that the significance of the non-resonant continuum contribution is 1.5σ only. Thus the default fit function does not include the continuum contribution. The fit results for the default model are given in Table 3.

The $\pi h_b(1P)$ and $\pi h_b(2P)$ invariant mass distributions corrected for the reconstruction efficiency are shown in Fig. 3. The data do not follow a phase space distribution but populate the mass region of the $Z_b(10610)$ and $Z_b(10650)$ states. We find that the transitions are dominated by the intermediate $Z_b(10610)$ and $Z_b(10650)$ states, but the limited statistics do not allow a measurement of the contribution from each mode.

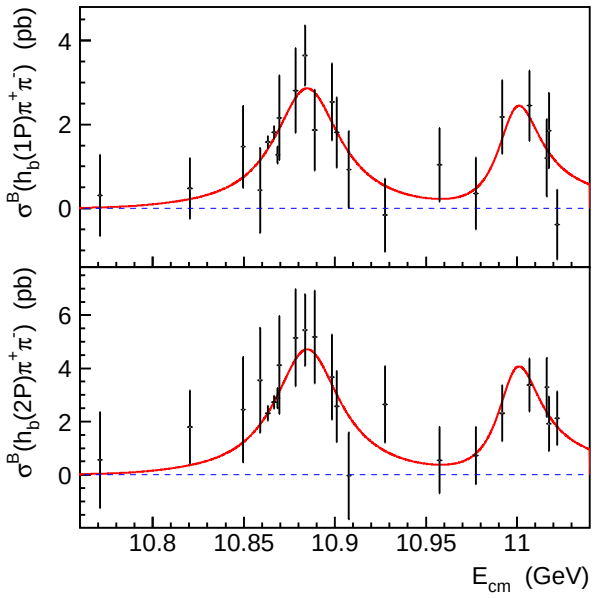


FIGURE 2. Cross sections for the $e^+e^- \to \pi^+\pi^- h_b(1P)$ (top) and $e^+e^- \to \pi^+\pi^- h_b(2P)$ processes as a function of CM energy. Points with error bars are the data, red solid curves are the fit results.

TABLE 3. Fit results for the default model.

Parameter	results
M_5 (MeV/c^2)	$10884.7^{+3.2+8.6}_{-2.9-0.6}$
Γ_5 (MeV)	$44.2^{+11.9+2.2}_{-7.8\ -15.8}$
M_6 (MeV/c^2)	$10998.6 \pm 6.1^{+16.1}_{-1.1}$
Γ_6 (MeV)	29^{+20+2}_{-12-7}
$A_1/10^3$	$4.8^{+2.7}_{-0.8}$
$A_2/10^3$	$8.0^{+4.6}_{-1.3}$
a	$0.64^{+0.37+0.13}_{-0.11-0}$
(ϕ/π)	$0.1^{+0.3}_{-0.5}$

CHARMMONIUM and CHARMONIUMLIKE STATES

The vector charmonium and charmoniumlike states are studied via ISR at Belle in the process $e^+e^- \to \gamma_{\rm ISR}\pi^+\pi^- J/\psi$ [8], $e^+e^- \to \gamma_{\rm ISR}\pi^+\pi^-\psi(2S)$ [9], and $e^+e^- \to \gamma_{\rm ISR}K^+K^- J/\psi$ [10]. Charged charmonium states decay into a charmonium and a charged pion (or a charged kaon) are searched for in the intermediate states.

$e^+e^- \to \pi^+\pi^- J/\psi$ and $Z_c \to \pi^\pm J/\psi$

The cross section for $e^+e^- \to \pi^+\pi^- J/\psi$ between 3.8 and 5.5 GeV is measured with a 967 fb^{-1} data sample collected by the Belle detector at or near the $\Upsilon(nS)$ (n = 1, 2, ..., 5) resonances [8]. Figure 4(a) shows the $\pi^+\pi^-\ell^+\ell^-$ invariant mass distributions after all of these selection requirements are applied and Fig. 4(b) shows the measured cross sections for $e^+e^- \to \pi^+\pi^- J/\psi$, where the error bars are statistical only.

The intermediate states in $Y(4260) \to \pi^+\pi^- J/\psi$ decays are also investigated [8]. The $Z(3900)^+$ state (is now called $Z_c(3900)$ after BESIII [11]) with a mass of $(3894.5 \pm 6.6 \pm 4.5)$ MeV/c^2 and a width of $(63 \pm 24 \pm 26)$ MeV is observed in the $\pi^\pm J/\psi$ mass spectrum (see Fig. 5) with a statistical significance larger than 5.2σ.

BESIII experiment studied the process $e^+e^- \to \pi^+\pi^- J/\psi$ at a CM energy of 4.260 GeV using a 525 pb^{-1} data sample [11]. The $Z_c(3900)$ is observed in the $\pi^\pm J/\psi$ mass spectrum with a statistical significance larger than 8σ. A fit to

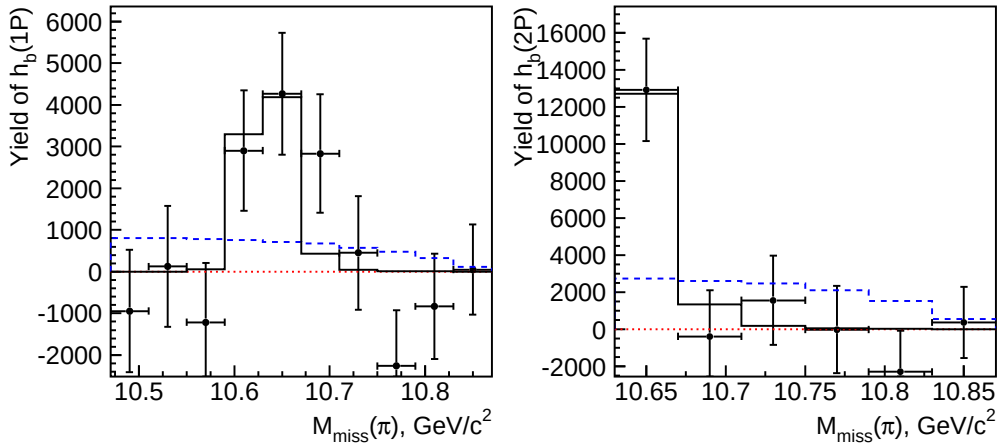


FIGURE 3. The efficiency corrected yields of $\pi^+\pi^- h_b(1P)$ (left) and $\pi^+\pi^- h_b(2P)$ (right) as a function of *pi* missing mass. Points represent data, the black solid histogram represents the fit result with the shape fixed from the $\Upsilon(5S)$ analysis, the blue dashed histogram is the result of the fit to the phase space distribution.

the $\pi^\pm J/\psi$ invariant mass spectrum (see Fig. 5), neglecting interference, results in a mass of $(3899.0\pm3.6\pm4.9)\,\mathrm{MeV}/c^2$ and a width of (46 ± 10 ± 20) MeV. The $Z_c(3900)$ was confirmed shortly after with CLEO-c data at a CM energy of 4.17 GeV [12], the mass and width agree with the BESIII and Belle measurements very well.

$e^+e^- \to \pi^+\pi^-\psi(2S)$ and $Z_c \to \pi^\pm\psi(2S)$

Using the 980 fb^{-1} full data sample taken with the Belle detector, the analysis of $e^+e^- \to \pi^+\pi^-\psi(2S)$ is updated with two $\psi(2S)$ decay modes [9], namely, $\pi^+\pi^- J/\psi$ and $\mu^+\mu^-$.

Fitting the mass spectrum of $\pi^+\pi^-\psi(2S)$ with two coherent BW functions (see Fig. 6), Belle obtains $M_{Y(4360)} = (4347\pm6\pm3)\,\mathrm{MeV}/c^2$, $\Gamma_{Y(4360)} = (103\pm9\pm5)\,\mathrm{MeV}$, $M_{Y(4660)} = (4652\pm10\pm8)\,\mathrm{MeV}/c^2$, $\Gamma_{Y(4660)} = (68\pm11\pm1)\,\mathrm{MeV}$. and $\mathcal{B}[Y(4360) \to \pi^+\pi^-\psi(2S)]\cdot\Gamma^{e^+e^-}_{Y(4360)} = (10.9\pm0.6\pm0.7)$ ev and $\mathcal{B}[Y(4660) \to \pi^+\pi^-\psi(2S)]\cdot\Gamma^{e^+e^-}_{Y(4660)} = (8.1\pm1.1\pm0.5)$ ev for one solution; or $\mathcal{B}[Y(4360) \to \pi^+\pi^-\psi(2S)]\cdot\Gamma^{e^+e^-}_{Y(4360)} = (9.2\pm0.6\pm0.6)$ ev and $\mathcal{B}[Y(4660) \to \pi^+\pi^-\psi(2S)]\cdot\Gamma^{e^+e^-}_{Y(4660)} =$ (2.0 ± 0.3 ± 0.2) ev for the other. Here, the first errors are statistical and the second systematic.

Since there are some events accumulating at the mass region of $Y(4260)$, the fit with the $Y(4260)$ included is also performed. In the fit, the mass and width of the $Y(4260)$ are fixed to the latest measured values at Belle [8]. There are four solutions with equally good fit quality. The signal significance of the $Y(4260)$ is estimated to be 2.1σ. The fit results are shown in Fig. 6 for one of the solutions. In this fit, one obtains $M[Y(4360)] = (4365 \pm 7 \pm 4)\,\mathrm{MeV}/c^2$, $\Gamma[Y(4360)] = (74 \pm 14 \pm 4)$ MeV, $M[Y(4660)] = (4660 \pm 9 \pm 12)\,\mathrm{MeV}/c^2$, and $\Gamma[Y(4660)] = (74 \pm 12 \pm 4)$ MeV.

Possible charged charmoniumlike structures in $\pi^\pm\psi(2S)$ final states from the $Y(4360)$ or $Y(4660)$ decays are searched for with the selected candidate events. Figure 7 shows $Y(4360)$ decays. An unbinned maximum-likelihood fit is performed on the distribution of $M_{\max}(\pi^\pm\psi(2S))$, the maximum of $M(\pi^+\psi(2S))$ and $M(\pi^-\psi(2S))$, simultaneously with both the $\pi^+\pi^- J/\psi$ and the $\mu^+\mu^-$ modes. We obtain a mass of $(4054 \pm 3(\mathrm{stat.}) \pm 1(\mathrm{syst.}))\,\mathrm{MeV}/c^2$ and a width of $(45 \pm 11(\mathrm{stat.}) \pm 6(\mathrm{syst.}))$ MeV for the $Z^\pm$ structure in the $\pi^\pm\psi(2S)$ system, and the statistical significance of the signal is 3.5σ. The $Y(4660)$ sample is very limited in statistics, and there is no significant structures in the $\pi^\pm\psi(2S)$ system.

$e^+e^- \to K^+K^- J/\psi$ and $Z_{cs} \to K^\pm J/\psi$

The cross section of the process $e^+e^- \to K^+K^- J/\psi$ are measured via ISR at CM energies between the threshold and 6.0 GeV using a data sample of 980 fb^{-1} collected with the Belle detector on or near the $\Upsilon(nS)$ resonances, where n =1, 2, ..., 5 [10]. The cross sections for $e^+e^- \to K^+K^- J/\psi$ are at a few pico-barn level as shown in Fig. 8. Possible intermediate states for the selected $K^+K^- J/\psi$ events are also investigated by examining the Dalitz plot but no

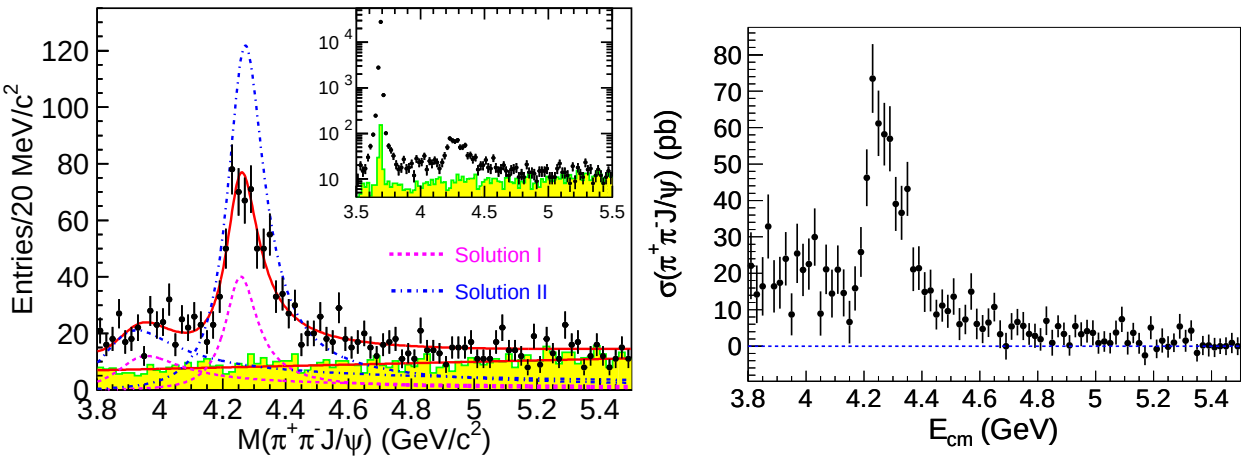


FIGURE 4. (Left) Invariant mass distributions of $\pi^+\pi^-\ell^+\ell^-$. Points with error bars are data, and the shaded histograms are the normalized J/ψ mass sidebands. The solid curves show the total best fit with two coherent resonances and contribution from background. The inset shows the distributions on a logarithmic vertical scale. The large peak around 3.686 GeV/c^2 is the $\psi(2S)\to\pi^+\pi^- J/\psi$ signal. (Right) Cross section of $e^+e^-\to\pi^+\pi^- J/\psi$ after background subtraction. The errors are statistical only.

clear structure is observed in the $K^\pm J/\psi$ system. A larger data sample is necessary to obtain more information about possible structures in the $K^+K^- J/\psi$, K^+K^- and $K^\pm J/\psi$ systems.

SUMMARY

There are lots of progress on the study of the quarkonium and quarkoniumlike states at Belle. The Belle II experiment [13] under construction, with about 50 ab^{-1} data accumulated, will surely improve our understanding of all these states.

ACKNOWLEDGMENTS

This work is supported in part by National Natural Science Foundation of China (NSFC) under contract Nos. 11235011 and 11475187; the Ministry of Science and Technology of China under Contract No. 2015CB856701, and the CAS Center for Excellence in Particle Physics (CCEPP).

REFERENCES

[1] A. J. Bevan *et al.* [BaBar and Belle Collaborations], "The Physics of the *B* Factories," Eur. Phys. J. C **74**, 3026 (2014).

[2] For a recent review, see N. Brambilla *et al.*, "Heavy quarkonium: progress, puzzles, and opportunities," Eur. Phys. J. C **71**, 1534 (2011).

[3] A. Abashian *et al.* [Belle Collaboration], Nucl. Instrum. Methods Phys. Res., Sect. A **479**, 117 (2002); also, see detector section in J. Brodzicka *et al.*, Prog. Theor. Exp. Phys. (2012) 04D001.

[4] S. Kurokawa and E. Kikutani, Nucl. Instrum. Methods Phys. Res., Sect. A **499**, 1 (2003), and other papers included in this volume; T. Abe *et al.*, Prog. Theor. Exp. Phys. (2013) 03A001 and following articles up to 03A011.

[5] D. Santel *et al.* [Belle Collaboration], "Measurements of $\sigma(e^+e^-\to\Upsilon(nS)\pi^+\pi^-)$ and $\sigma(e^+e^-\to b\bar{b})$ in the $\Upsilon(10860)$ and $\Upsilon(11020)$ resonance regions," arXiv:1501.01137 [hep-ex].

[6] A. Garmash *et al.* [Belle Collaboration], "Amplitude analysis of $e^+e^-\to\Upsilon(nS)\pi^+\pi^-$ at $\sqrt{s}$ = 10.865 GeV," Phys. Rev. D **91**, no. 7, 072003 (2015).

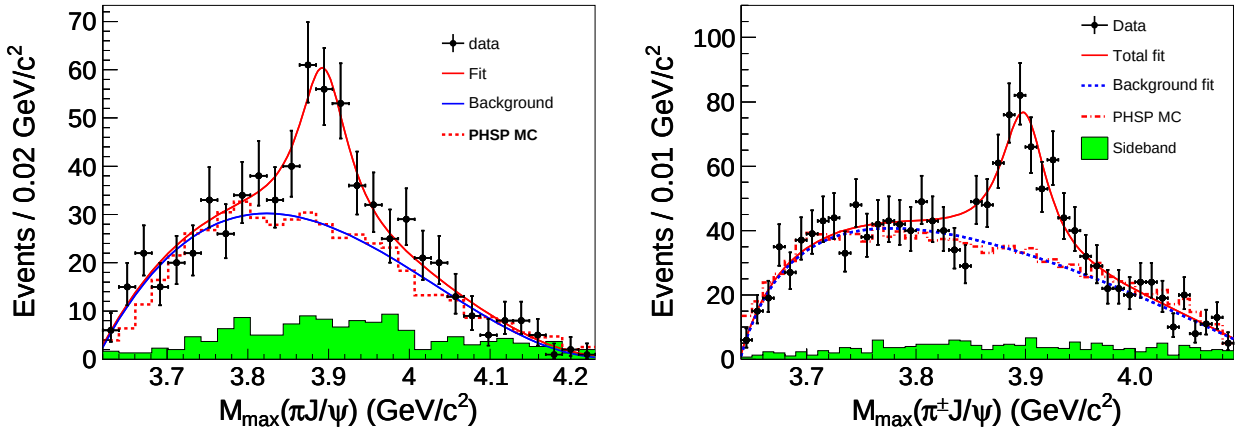


FIGURE 5. Unbinned maximum likelihood fit to the distribution of the $M_{\rm max}(\pi J/\psi)$ (left panel from Belle and right panel from BESIII). Points with error bars are data, the curves are the best fit, the dashed histograms are the phase space distributions and the shaded histograms are the non-$\pi^+\pi^- J/\psi$ background estimated from the normalized J/ψ sidebands.

[7] A. Abdesselam *et al.* [Belle Collaboration], "Energy scan of the $e^+e^- \to h_b(nP)\pi^+\pi^-$ ($n = 1, 2$) cross sections and evidence for the $\Upsilon(11020)$ decays into charged bottomonium-like states," arXiv:1508.06562 [hep-ex].

[8] Z. Q. Liu *et al.* [Belle Collaboration], "Study of $e^+e^- \to \pi^+\pi^- J/\psi$ and Observation of a Charged Charmoniumlike State at Belle," Phys. Rev. Lett. **110**, 252002 (2013).

[9] X. L. Wang *et al.* [Belle Collaboration], "Measurement of $e^+e^- \to \pi^+\pi^-\psi(2S)$ via Initial State Radiation at Belle," Phys. Rev. D **91**, no. 11, 112007 (2015).

[10] C. P. Shen *et al.* [Belle Collaboration], "Updated cross section measurement of $e^+e^- \to K^+K^- J/\psi$ and $K^0_S K^0_S J/\psi$ via initial state radiation at Belle," Phys. Rev. D **89**, no. 7, 072015 (2014).

[11] M. Ablikim *et al.* [BESIII Collaboration], "Observation of a Charged Charmoniumlike Structure in $e^+e^- \to \pi^+\pi^- J/\psi$ at $\sqrt{s} = 4.26$ GeV," Phys. Rev. Lett. **110**, 252001 (2013).

[12] T. Xiao, S. Dobbs, A. Tomaradze and K. K. Seth, "Observation of the Charged Hadron $Z_c^{\pm}(3900)$ and Evidence for the Neutral $Z_c^0(3900)$ in $e^+e^- \to \pi\pi J/\psi$ at $\sqrt{s} = 4170$ MeV," Phys. Lett. B **727**, 366 (2013).

[13] T. Abe *et al.* [Belle-II Collaboration], "Belle II Technical Design Report," arXiv:1011.0352 [physics.ins-det].

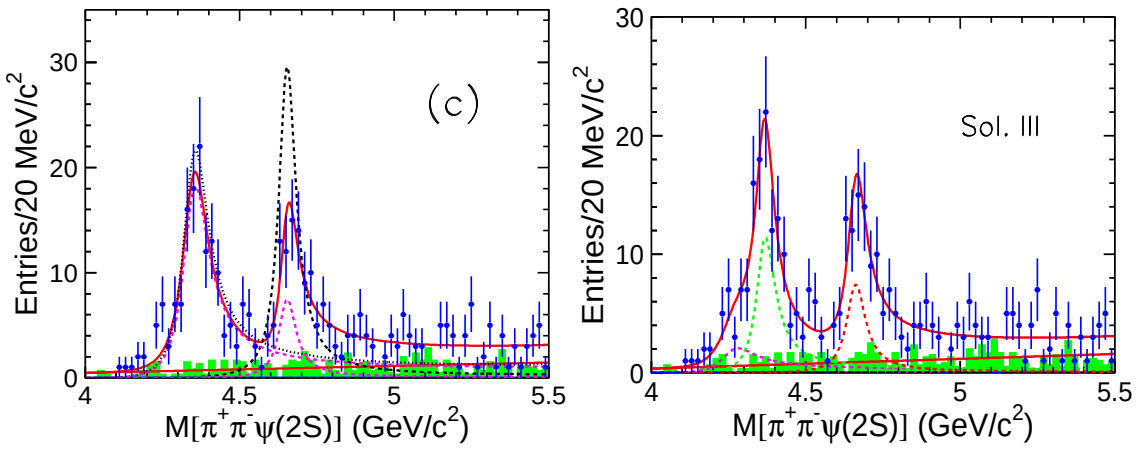


FIGURE 6. The $\pi^+\pi^-\psi(2S)$ invariant mass distribution from the Belle experiment and the fit results with the coherent sum of two BW functions (left) and three BW functions (right). The sum of $\pi^+\pi^- J/\psi$ and $\mu^+\mu^-$ modes is shown. The points with error bars are data while the shaded histograms the normalized $\psi(2S)$ sideband backgrounds. The curves show the contributions from different BW components.

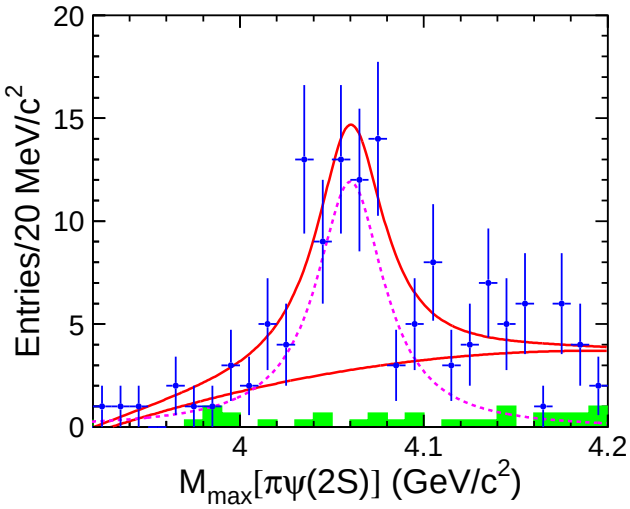


FIGURE 7. The distribution of $M_{\rm max}(\pi^\pm\psi(2S))$ from $Y(4360)$-subsample decays. The points with error bars represent the data; the histogram is from the sidebands and normalized to the signal region; the solid curve is the best fit and the dashed curve is the signal parameterized by a BW function.

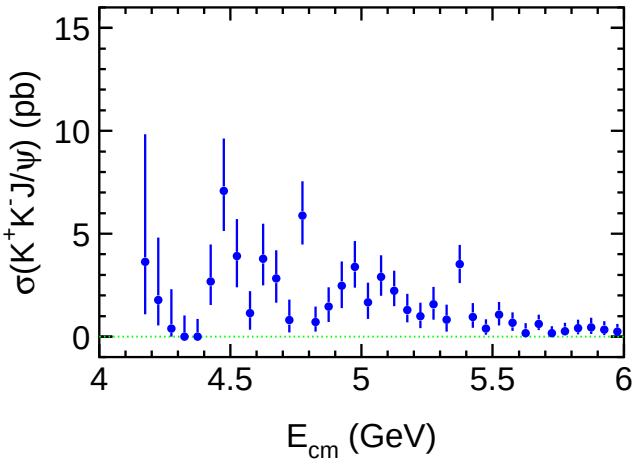


FIGURE 8. The measured $e^+e^- \to K^+K^-J/\psi$ cross sections for CM energies up to 6.0 GeV (points with error bars). The errors are statistical and a 7.8% systematic error that is common for all data points is not included.